Sara Rios, Nuno Cristelo, Tiago Miranda, Nuno Araújo, Joel Oliveira &
Ernesto Lucas (2016): Increasing the reaction kinetics of alkali-activated fly ash binders for stabilisation of a silty sand pavement sub-base, Road Materials and Pavement Design, DOI: 10.1080/14680629.2016.1251959

http://dx.doi.org/10.1080/14680629.2016.1251959

Increasing the reaction kinetics of alkali activated fly ash binders for stabilisation of a silty sand pavement sub-base

[a,*] Sara Rios; [b] Nuno Cristelo; [c] Tiago Miranda; [d] Nuno Araújo; [e] Joel Oliveira; [d] Ernesto Lucas

[a] *Post-Doc Research fellow, CONSTRUCT-GEO, Department of Civil Engineering, Faculty of Engineering, University of Porto, 4200-465 Porto, Portugal*
[*] Corresponding author
E-mail address: sara.rios@fe.up.pt

[b] *Assistant Professor, CQVR, Department of Engineering, University of Trás-os-Montes e Alto Douro, 5001-801 Vila Real, Portugal*

[c] *Assistant Professor, ISISE, Department of Civil Engineering, University of Minho, 4800-058 Guimarães, Portugal*

[d] *Assistant Professor, ISISE, Department of Civil Engineering, University of Minho, 4800-058 Guimarães, Portugal*

[e] *Assistant Professor, CTAC, Department of Civil Engineering, University of Minho, 4800-058 Guimarães, Portugal*

[d] PhD student, *CQVR, Department of Engineering, University of Trás-os-Montes e Alto Douro, 5001-801 Vila Real, Portugal*

Abstract

The paper addresses several options to improve the reaction kinetics of alkali activated low calcium fly ash binders for soil stabilisation in road platforms. For that purpose, an experimental program was established to assess the strength evolution, with time, of different binders, based on ash, lime, sodium chloride and alkali solutions, applied in the stabilisation of a silty sand. The tests included unconfined compression strength tests, triaxial tests and seismic wave measurements performed at different curing periods. The results were compared with a binder made of Portland cement and a commercial additive specifically designed for soil stabilization in road applications. The activated ash mixtures with lime were the most performing producing a significant increase in the reactions development and, consequently, in the strength gain rate. The sodium chloride significantly improved the lime and lime-ash mixtures, but provided only a slight improvement in the activated ash mixtures.

Keywords: soil stabilization; fly ash; lime; alkaline activation, Portland cement

Introduction

With the worldwide increase in constructed surface area, the need for local soil stabilization or improvement keeps growing. Different methods have been used for decades, and several of those are still being improved and refined, while new ones keep arising as technology progresses. According to Mitchell (1981) and van Impe (1989) the stabilisation / improvement techniques can be divided in the following groups: consolidation; grouting; mechanical, chemical and physical stabilisation; and soil reinforcement. Almost all of the mentioned groups comprise one or more techniques that can be very efficiently applied in transport infrastructures. Compaction, consolidation, grouting and soil reinforcement can be used to improve the bearing capacity and deformability properties of embankments or slopes; while mechanical (surface compaction) and chemical stabilisation are very common when dealing with superficial layers.

In particular, chemical stabilisation is very efficient when the soils available nearby cannot present an adequate performance based only on mechanical stabilisation. The use of a soil-binder combination specifically developed for subgrade layers can significantly increase its strength and stiffness, avoiding the extraction of more performing materials from distant locations (Ingles & Metcalf, 1972; Little, 1995; Sherwood, 1993; Little & Nair, 2009).

The most common binders for surface stabilisation are based on Ordinary Portland cement (OPC) and/or lime (Petry & Little, 2002; Xing et al, 2009). Due to the pozzolanic properties of common clay minerals, the high amount of calcium present in both slaked and unslaked lime makes it a very effective option to decrease plasticity and increase workability, with also some significant strength and stiffness increase if dry weight percentages above 6% are used (Cristelo et al, 2009; Little et al, 2010; Al-Mukhtar et al, 2014; Gullu, 2015; Han & Cheng, 2015; Elkady, 2016). When dealing with silty to sandy soils, OPC is usually the most interesting option (Consoli et al, 2011a; Bahar et al, 2004; Goodary et al, 2012; Rios et al., 2012, 2014). However, if a significant increase in strength is necessary in a clayey soil, the

most consensual strategy is probably to mix the soil with lime, before mixing the resulting granular material with OPC (Horpibulsuk et al., 2006; Yusuf et al, 2001; Yong & Ouhadi, 2007; Oza & Gundaliya, 2013; Khemissa and Mahamedi, 2014; Saride et al, 2013). Several binders have been tested, with more or less success (Kolias et al, 2005; Basha et al 2005; Kaniraj & Havanagi, 1999; Kamei et al, 2013; Yilmaz & Ozaydin, 2013; Gurbuz et al, 2015), but in almost every case OPC plays a major role in the stabilisation process.

Based on the literature review, it becomes clear that cement is the most important constituent in chemical stabilisation of soil subbases, producing significant strength and stiffness increase with little or no setbacks whatsoever. Nevertheless, the decreasing tolerance regarding the environmental concern has the production of clinker as a major target, mostly due to the high amount of CO_2 released. A value between 5% and 8% of the overall CO_2 released to the atmosphere is estimated to be originated by OPC production (Provis & van Deventer, 2014; Scrivener & Kirkpatrick, 2008). Therefore, there is an ongoing research effort targeting the development of more sustainable binders (Juenger et al., 2011). In particular, the use of waste materials is highly encouraged, since it allows an increase in resource efficiency, while contributing also to enhancing the circular economy (by reducing landfilled waste).

The alkaline activation technique is particularly adequate to create binders based on residues, such as fly ash or ground granulated blast furnace slag, which constitute very effective options due to their amorphous aluminosilicate microstructure. It consists on a reaction between aluminosilicate materials and alkali or alkali-based earth substances, such as sodium (Na) or potassium (K), or an alkaline earth ion, such as calcium (Ca). The reactions can be summarized in the following sequence. First, there is the destruction, by the high hydroxyl (OH-) concentration in the alkaline medium, of the Si-O-Si, Al-O-Al and Al-O-Si covalent bonds present in the vitreous phase of the original semi-amorphous aluminosilicate (i.e. the precursor). The Si and Al ions are released into the solution as they become available

and; at the same time, the alkaline cations – usually Na+ or K+, depending on the activator – compensate the excess negative charges associated with the modification of the aluminium coordination during the dissolution phase. The resulting products accumulate for a period of time, forming an ion-rich solution, which finally precipitates and reorganizes into more stable and ordered Si-O-Al and Si-O-Si structures. If calcium is predominant, relatively to the sodium or potassium, the dissolved Al-Si ions will diffuse from any solid surface, which favours the production of a C-S-H gel phase. Otherwise, the Si and Al ions will be able to accumulate around the nuclei points, sharing all the oxygen ions and forming a Si-O-Al and Si-O-Si three-dimensional structure (the formation of Al-O-Al is not favoured). The resulting product is an amorphous alumina-silicate gel, which evolves, with curing time and crystallization, from an Al-rich phase to a Si-rich phase. The crystallization, starting almost immediately after the precipitation, is responsible for the hardening of the gel, which eventually matures into alkaline cement, with pre-zeolite as secondary products (Fernández-Jiménez and Palomo, 2005; Fernández-Jiménez et al., 2006). The precursor should always be submitted to a previous thermal treatment, capable of inducing the loss of constituent water and the subsequent re-coordination of the aluminium and oxygen ions, transforming an originally crystalline structure into an amorphous one, more susceptible to further chemical reactions. The relative presence of calcium in the precursor and/or in the activator is very important, since the speed of the reactions is highly dependent on the type of aluminosilicate gel being formed, either N-A-S-H or C-S-H. The former needs longer periods in order to mature into a stable and reliable matrix, while the latter has curing / developing periods similar to those obtained with cement-based binders (Dombrowski et al, 2007; Garcia-Lodeiro et al., 2013).

Alkaline activation has recently started to be applied in soil stabilisation applications, using fly ash as the precursor, allowing significant strength gains (Zhang et al, 2013; Sukmak et al., 2013, 2015; Cristelo et al., 2011, 2012a, 2013; Silva et al., 2013; Rao and Acharya,

2014; Yi et al., 2015; Rios et al., 2015; Phummiphan et al., 2016), but also financial and environmental benefits, which proved very competitive when compared with lime or cement-based soil stabilizers (Cristelo et al., 2015). Other works were also recently published using alkaline activation to stabilise other types of granular materials that do not include soils such as construction and demolition waste (Mohammadinia et al., 2015; Arulrajah et al., 2016), coffee grounds (Kua et al., 2016), or recycled asphalt pavement (Saride et al., 2016, Hoy et al., 2016). However, constrains related with short deadlines regarding the entry into operation of most infrastructures, and namely road and railways, often require tight construction periods, which hinders the use of alkali activated low calcium (class F) fly ash, based on the mentioned slower reaction kinetics of the N-A-S-H gel, when compared with the C-S-H gel. However, in the presence of enough calcium, the two systems are very compatible, and several studies have focused on the characterisation of their interaction and coexistence (Garcia-Lodeiro et al., 2009, 2011; Puligilla & Mondal, 2013; Bui et al, 2015).

The need to improve the reaction kinetics of alkali activated class F fly ash binders constituted the motivation of the present paper. A viable method would have been the use of activated class C (high calcium) fly ash, which has proved very efficient for the stabilisation of a lateritic soil for bound pavement application (Phummiphan et al., 2016). However, assuming that such high calcium fly ash is not available, the need to develop alternative procedures to increase the strength gain rate is obvious. Therefore, several mixtures were prepared to find an effective method to increase the strength gain rate of a silty-sand stabilised with low calcium, alkali activated fly ash.

Some authors (Ghosh and Subarao, 2001; Kumar et al., 2007; Samaras et al., 2008; Consoli et al., 2011b) have reported that a significant strength increase of lime stabilised clayey soils can be achieved with the addition of fly ash, enhancing the pozzolanic reaction, which is the main responsible for the mechanical properties of the soil-lime mixture. Additionally, several authors (Ramesh et al., 1999; Narendra et al., 2003; Cristelo et al., 2009)

have concluded that the formation of such pozzolanic reaction compounds is faster in the presence of sodium chloride. According to these authors, this can be attributed to the increased solubility of the silica and to the formation of sodium calcium silicate hydrate (N-S-C-H), more voluminous and with a higher water-holding capacity than the well-known C-S-H gel, formed in the sole presence of soil and lime. Based on these findings regarding the role of fly ash and sodium chloride on soil stabilisation, additional mixtures were considered, for comparison purposes, in which fly ash was added to soil-lime mixtures, with and without the addition of sodium chloride. The addition of sodium chloride was also used to prepare activated fly ash mixtures. Finally, a specific commercial additive for road pavement applications (recently available in the market called RoadCem®) was mixed with Portland cement, and the resulting binder was used to prepare some additional specimens. The result was regarded as a threshold value to which the mixtures developed in the present work were compared with.

In short, the following mixtures were conceptually analysed throughout the paper:

- Lime alone and with sodium chloride;
- No-activated fly ash and lime with and without sodium chloride;
- Activated ash and lime with and without sodium chloride;
- RoadCem® and Portland cement

Experimental program

Soil identification

The work presented in this paper was based on a soil from Poland, which was fully characterized at the beginning of the experimental program described below. Typical geotechnical identification tests were performed in order to determine the particle size

distribution, Atterberg's limits, Modified Proctor compaction parameters, and the California Bearing Ratio (CBR). The particle size distribution curve (Figure 1) evidences a well graded soil, with almost 50% fines – silt (27.8%) and clay (16%), which was classified as a SC-SM - silty sand according to ASTM (2011) D 2487-11. Other parameters are summarised in **Erro! A origem da referência não foi encontrada.**.

The minerology was examined by a PANalytical X'Pert Pro diffractometer, fitted with an X'Celerator detector and secondary monochromator. The scans covered a 2 Θ range of 10º to 80º, with a nominal step size of 0.017º and 100 s/step. CuK α radiation, with a wavelength of λ =1.5418 Å, was used. Qualitative phase identification was made using High Score Plus software, which utilises the International Centre for Diffraction Data Power Diffraction File database (ICDD PDF-2, Sets 1-49, 1999) as a reference. X-Ray diffraction patterns of the soil showed the presence of quartz and muscovite on the mineralogical composition.

Characterisation of the binders

The fly ash was provided by a Portuguese thermo-electric power plant and, based on ASTM C 618 (2015), was classified as Class F due to the low calcium content as it is expressed on Table 2. Hydrated lime provided by the company Lusical, Lhoist was also used. The particle size distribution of both lime and fly ash are plotted in Figure 1 together with the soil particle analysis. The activator solution used was composed by sodium hydroxide and sodium silicate . The former was supplied in pellets, with a specific gravity of 2.13 at 20ºC (99 wt. %), as indicated by the supplier, which was then dissolved in water to pre-determined concentration of 12.5 molal. The sodium silicate technical sheet indicates a unit weight of 1.464 g/cm^3 at 20ºC, a SiO_2/Na_2O weight ratio of 2.0 (molar oxide ratio of 2.063) and a Na_2O concentration in the solution of 13.0%. A sodium silicate to sodium hydroxide ratio of 0.5 was always considered. Deionised water was used in every mixture prepared during the work presented.

Some mixtures were also prepared with Ordinary Portland cement, type CEM I-42.5R, together with a commercial soil stabiliser, specifically designed for road pavements, named RoadCem®. This product can be described as a fine grain additive, based on alkali earth metals and synthetic zeolites, complemented with a complex activator. Based on the technical sheet, this product modifies and extends the chemistry of the cement hydration process and extends the crystallization process by forming long needle crystalline structures. It is able to delay or to speed up the hydration process of cement and can thus be used as a tool to custom design the mixes of required performance. It is always used in combination with cement and/or other pozzolanic materials (Marjanovic et al., 2009).

Specimen preparation and mixture composition

Preparation of the soil included drying and de-flocculation by hand. The solids were then dry mixed for 10 min in a Hobart counter mixer, and the liquid phase was carefully added, requiring an additional 10 min mixing period. Cylindrical specimens with 70 mm in diameter and 140 mm in height were then compacted for uniaxial and triaxial compression strength tests, using static compaction according to EN 13286-53 CEN (2004a). The top and bottom of the moulds were then covered with cling film and the specimens were left for forty-eight hours before the mould could be removed. After demoulding the specimens were allowed to cure for longer in the same conditions: at 20ºC ± 1ºC and 90% RH ± 3%.

Identification of the mixtures is presented in **Erro! A origem da referência não foi encontrada.**. Each component of the solid phase is defined as a percentage of the total mass of solids, and the water content as the ratio between the amount of water and the amount of solids. All mixtures were identified using the following code: ‘S’ (soil); ‘FA’ (fly ash); ‘L’ (lime); ‘C’ (sodium chloride); ‘AA’ (alkali activated); ‘OPC’ (Ordinary Portland cement) and ‘RC’ (RoadCem). Some of these letters were followed by a number, indicating the respective dosage. In the first step the specimens were moulded on the maximum dry unit weight and

optimum water content, obtained for the soil, using a modified Proctor test (**Erro! A origem da referência não foi encontrada.**), but in the second and third steps the presence of lime and the consequent cationic exchange and flocculation prevented a higher compaction degree. Therefore, in steps 2 and 3, mixtures were moulded at 88% of the optimum dry unit weight, corresponding to a maximum dry unit weight of 18.8 kN/m^3. All specimens were moulded with a water content of 5%, corresponding to 88% value in the Proctor curve, with the exception of the geopolymeric mixtures, which required a higher water content in order to fulfil the criteria related with the activator/ash ratios. For comparison purposes, a specimen of unstabilised soil was also prepared, being compacted at 88% of the Proctor maximum value.

Uniaxial compression strength testing

An Instron® electro-mechanical load frame , fitted with a 25 kN load cell, was used for the unconfined compressive strength tests. The tests were carried out according to EN 13286-41 (CEN, 2003a) under monotonic displacement control, at a rate of 2 mm/s, and the entire stress-strain curve was obtained from each test.

Triaxial testing

Consolidated undrained triaxial compression tests (CU), following CEN ISO/TS 17892-9 (CEN, 2004b), were performed on the original soil, after isotropic effective consolidation stresses (σ'_c) of 33 kPa, 100 kPa and 300 kPa. Additionally, drained triaxial compression tests (CD) were performed in two of the bounded mixtures – S_FA15_L5_AA3 and S_FA10_L5_AA3 – previously cured for 28 days, using effective isotropic consolidation stresses of 50 kPa, 100 kPa and 200 kPa. These particular mixtures were chosen due to the fact that they reached the most performing behaviour in the UCS tests.

After the installation in the triaxial cell, water was allowed to percolate through the specimen until a volume of water higher than twice the volume of voids was obtained. This

facilitated saturation because removed the air bubbles present in the specimen and in the tubing system. Then, the saturation followed where cell and back pressures were increased simultaneously at a rate of 30 kPa per hour keeping an effective stress of 10 kPa, until cell and back pressure achieved 410 and 400 kPa respectively. This back-pressure value was kept constant during 24 h, assuring full-saturation which was verified by the B Skempton parameter which was close to 1.

The same servo-hydraulic load frame used for UCS tests, fitted with a 25 kN load cell, was used to apply the deviatoric load, under monotonic displacement control, at a rate of 0.01 mm/min. The axial deformation was measured by two Linear Displacement Transformers (LDTs) (Goto et al., 1991), while an additional LDT was installed to monitor the radial deformation as illustrated in Figure 2.

Seismic waves

Compression seismic (P) wave velocities were measured by ultrasonic non-destructive transducers, after curing periods of 12, 24 and 48 h, and then after 3, 7, 14 and 28 days in some of the specimens tested in unconfined compression as expressed in **Erro! A origem da referência não foi encontrada.**. A commercially available equipment was used, consisting of axially aligned piezoelectric transducers, with a nominal frequency of 54 kHz and 30 mm in diameter; a waveform generator; an amplifier and an interval timer with a direct reading digital display, which showed the P-wave velocity (V_P) in real time. An oscilloscope would have been preferable, due to the lower definition of the pulse wave when travelling through heterogeneous materials, like soil. However, such equipment was not available. The equipment has an excitation voltage of 1000V and a resolution of 0.1μs. The equipment identified automatically the P wave travel time without any operator interference, and therefore no specific analysis was needed as in other advanced devices (Camacho-Tauta et al., 2015). In this case, standard EN 12504-4 (CEN, 2003b) was used as general reference, and

calibration of the transducers was automatically performed by the equipment, using a metallic rod with a known P-wave travelling time of 20.9μs. The measurements were taken along the longitudinal axis of the specimens, with the specimen vertically aligned and the transducers installed on opposite faces. The acoustic coupling between the transducers and the specimen was obtained using ultrasound gel, while firmly pressing the transducers against the top surfaces of the specimen. Each result presented is the average of ten consecutive readings.

Experimental results

Unconfined compressive strength

In the first step of **Erro! A origem da referência não foi encontrada.**, designed to obtain a guideline in terms of time needed for the reaction to produce meaningful UCS results, three different liquid/solids ratios were considered, by varying the liquid phase (the solids were kept at 85% S + 15% FA). Based on the results obtained, further activated mixtures were performed with an activator / ash ratio equal to 0.707 (the criteria for such value are discussed later in the text).

In the second step, the soil was mixed with different binders in order to evaluate the effect, on the reaction's kinetics, of each of the combinations proposed. Mixtures of soil-lime as well as soil-lime-fly ash (both with and without sodium chloride) were first performed with deionised water as the only constituent of the liquid phase. Then, the fly ash and fly ash-lime mixtures were prepared with the activator as the only constituent of the liquid phase.

A third and final step was then designed to reduce the mixture cost which included the reduction of the fly ash to 10% of the total solids (and consequently, a lower quantity of activator solution), while using only one lime percentage (10%) and 1% of sodium chloride. Also included in this final step were the OPC + RC mixtures.

304 At least 3 specimens of each condition were always moulded and tested so that the
305 presented data corresponds to the average of three tests, improving the statistical confidence
306 on the results. A unique curing period of 28 days was considered during the first step, while
307 three different curing periods of 3, 7 and 28 days were considered in the second step. In the
308 third step, L + FA specimens were tested after 7 days, while OPC + RC specimens were cured
309 for 3, 7 and 28 days as expressed in **Erro! A origem da referência não foi encontrada.**

310 The results obtained in step 1 with distinct activator contents and a ash content of 15% was
311 aimed to evaluate the effect of the Na_2O/ash ratio on UCS (Cristelo et al., 2012a). As such,
312 activator/ash ratios of 0.943, 0.825 and 0.707 were considered, resulting in activator contents
313 (liquid/solids ratio) of 14.1%, 12.4%, and 10.6%. Since the three mixtures presented a
314 significant strength increase (Figure 3), the lowest activator content of 10.6% was selected for
315 the following steps, even though the activator content of 12.4% achieved higher strength. This
316 was due to the fact that a reduction in activator implies a reduction of the total cost of the
317 mixture, since the activator is, by a significant margin, the most expensive component.

318 Figure 4 illustrates the strength results obtained in step 2, as well as the corresponding secant
319 stiffness modulus at 50% of the maximum strength (E_{50}). This parameter is essential to
320 characterise the material's constitutive model included in any finite element code, and
321 therefore its calculation is extremely useful for design purposes. With a few exceptions, the
322 mixtures with lower and higher strength values presented also lower and higher stiffness
323 values, respectively. Mohammadinia et al. (2014) have reported a E_{50}/UCS ratio around 1000
324 for cement-treated construction and demolition materials but in this case the ratio is closer to
325 100 probably due to a finer grading of the soil.
326 Note the significantly higher strength, after every curing period, achieved by the
327 mixtures with both lime and activated ash. While the mixture with activated ash achieved
328 similar strength values to those obtained by the lime and lime-fly ash mixtures, the addition of

lime to the former resulted in a 4 times strength increase. This is a consequence of the faster reactions in C-S-H systems, relatively to N-A-S-H systems, as observed by the authors Cristelo et al. (2012b) during a previous work that compared the strength gain rate motivated by the activation of class C and class F fly ash.

Considering the existing design guidelines for roads, both the Portuguese road specifications (JAE, 1995) and the French (GTS, 2000) classification chart for soil-cement mixtures, suggest a minimum indirect tensile strength of 0.2 or 0.3 MPa, depending whether in situ or plant mixing is used. These values can be converted into UCS values of 2 and 3 MPa assuming a ITS/UCS=10%. The GTS (2000) specification also adds the need to have 1 MPa at 7 days of curing. Using these values as target for design, as expressed in Figure 4, it becomes clear that the soil-lime mixture do not fulfil these aims, while the soil-lime-ash mixtures stay slightly above these limits. For higher performances, corresponding to higher class treated layers as expressed in GTS (2000), activated ash mixtures are needed.

A final third step was conducted to address the possible reduction of the economic and financial cost of the binders, considering that most UCS values obtained were very satisfactory and could be slightly reduced without compromising its mechanical performance. This cost decrease was obtained with a reduction of the fly ash percentage to 10%, down from the step 2 overall value of 15%. Note that a reduction in fly ash content does not represent a significant economic or environmental saving, but the reduction of the alkaline solution content needed to activate the fly ash is, indeed, significant in terms of both of these aspects. Results presented in Figure 5 (after curing for 7 days) show that the mixtures with both lime and activated ash remain as the most performing combinations, even relatively to those mixtures based on both cement and RoadCem®.

Triaxial compression strength

Figures 6 and 7 show the stress-strain curves obtained from the triaxial tests performed on the

soil and selected bounded mixtures (with lime and activated ash), respectively as indicated in **Erro! A origem da referência não foi encontrada.**. These soil-binder mixtures were selected based on the efficiency/cost ratio obtained from the results from the uniaxial compression tests presented above.

The soil presented a quasi-linear behaviour up to 29%, 27% or 14% of the maximum deviatoric stress, depending on the effective confining pressure applied of 33, 100 or 300 kPa, respectively. After this linear segment, the soil stiffness significantly decreases, due to yielding, reaching a zero value when the soil achieved a constant stress plateau at the 20% to 30% strain mark. **Erro! A origem da referência não foi encontrada.** presents the results of the stiffness modulus at 50% of the maximum deviatoric stress (E_{50}), a usual design parameter as explained before.

The bounded mixtures showed completely different stress-strain curves, which in this case are typical of cemented materials (Rios et al., 2014, 2015), with a peak stress at very low strain levels (between 0.15 and 0.30%), followed by a very abrupt strain softening due to bond degradation. The material stiffness does not seem to be very much affected by the effective confining pressure, indicating that, for this pressure range, the consolidation stress did not produce an increase in stiffness, but it did not damaged the cemented structure either. This behaviour, typical of cemented soils (e.g., Fernandez and Santamarina, 2001), is expressed in **Erro! A origem da referência não foi encontrada.** showing that the E_{50} stiffness modulus was very similar for the three tests on S_FA10_L5_AA3 specimens (approximately 3000 MPa) and also for the three tests on S_FA15_L5_AA3 specimens (approximately 4000 MPa). Note that the latter E_{50} value is almost 10 times higher than the values obtained with the unstabilized soil. Also very clear is the fact that the reduction in ash content (from 15% to 10%), had a strong influence on peak stress, which decreased between 30% to 40%, depending on the confining pressure.

P-wave measurements

The results obtained from the seismic wave measurements are presented in Figure 8 relating the P wave velocity (V_P) with curing time. It should be noted that the specimens are not saturated, and so the presented results do not represent the propagation velocity through the water, but through the soil grains. Consequently, the positive evolution of V_P with curing time is expected since V_P are directly related with the constrained modulus being therefore an indirect measurement of stiffness. The relative position between the V_P values obtained in each specimen is in agreement with the previous data presented in Figure 4, confirming the sensibility of this measurement.

However, the major advantage of this data is that being a non-destructive method it is possible to have several measurements through the curing period without needing further specimens. Figure 8 shows that there is a significant improvement in the first 7 days of curing and then the evolution continues at a smaller rate. This is especially relevant for alkali-activated ash mixtures and for specimens with lime and sodium chloride.

Discussion

Strength envelope of bounded and unbounded mixtures

The strength increase resulting from the mixture with lime and activated ash can be quantified in terms of the Mohr Coulomb failure criterion, namely from the resulting strength parameters ϕ' (friction angle) and c' (cohesion). The peak and ultimate strength envelopes of the soil and the selected bounded mixtures are presented in Figure 9, while the corresponding Mohr-Coulomb parameters are summarized in **Erro! A origem da referência não foi encontrada.**. It is possible to observe that the peak friction angle almost doubled, while the peak cohesion intercept suffered also a significant increase, which is typical of cemented materials. At

403 ultimate states the strength of the bounded mixtures approaches that of the soil since the
404 cohesion intercept reduces drastically. However, the values of the ultimate state friction angle
405 are still significantly higher than those obtained for the unstabilized soil (peak or ultimate
406 state). This indicates that not all the artificially created bonds could be destroyed in the test,
407 instead forming small clusters that reduced the void volume between the soil particles.

408 ***Effect of sodium chloride addition***

409 Figure 10 presents the Step 2 UCS related to the sodium chloride addition. The sodium
410 chloride was particularly effective in increasing the strength development rate of the non-
411 activated ash mixtures (S_L5 and S_FA15_L5), particularly after 28 days. The contribution of
412 the sodium chloride to the reaction kinetics is clear and, after 28 days, the addition of 1%
413 represents an UCS increase of 69% of the lime-based mixture and 59% of the lime and no-
414 activated ash mixture. Regarding the activated ash mixtures (S_FA15_L5_AA3), it appears
415 that the sodium chloride did not make a noticeable impact on strength increase, and has even
416 hindered the short-term (3 days) behaviour.

417 ***Effect of lime percentage***

418 Step 2 tests also allowed to observe the effect of hydrated lime on the reaction kinetics of the
419 mixtures. Figure 11 compares the strength values obtained for the two lime percentages
420 considered (5% and 10%), for each of the three curing periods. The results indicate that the
421 increase in lime content affects the rate of strength development, especially between the 7th
422 and the 28th day. An increase of 5% in lime content, after 28 days curing, represented
423 strength increases of 40% (soil + lime + water), 56% (soil + ash + lime + water) and 22%
424 (soil + ash + lime + activator).

Effect of ash percentage

Comparing step 2 and step 3 UCS results, after 7 days curing, it is possible to evaluate the effect of the fly ash content – 0%, 5% and 10% of the total solids weight (Figure 12). Overall, the results are in agreement with those from the triaxial tests presented before, where it was clear that the reduction in ash content (from 15% to 10%) represents a decrease in strength. This decrease is significantly more pronounced when the ash is activated, at least after 7 days curing.

On the other hand, it is interesting to note that the use of lime and 10% fly ash represents a strength decrease relatively to the use of lime alone. This is contrary to the results of Consoli et al. (2011b), that reported a significant strength increase when 12,5% and 25% ash were added to distinct lime percentages (from 3% to 9%), when stabilizing a similar soil, using very similar fly ash, in terms of chemical composition. This suggests the possibility of existing a minimum ash content in order to take full advantage of the pozzolanic effect of the ash. On the other hand, pozzolanic effects on strength require an extended curing period to be fully noticeable. It is possible that, for higher curing periods (when there is enough time to take full advantage of the added fly ash), the strength of the soil + lime + ash + water mixtures will increase linearly with the ash content. This is not noticeable at this early curing period of 7 days, where the overall particle size distribution might be prevalent in terms of UCS. Assuming that this second hypothesis is indeed correct, the gap between activated and non-activated mixtures will probably be reduced with time. Although both mixtures have ash and calcium required to develop pozzolanic reactions, in the case of the activated mixtures there is also a N-A-S-H gel type forming, which will hinder the development of calcium-based reactions after medium to long term curing periods.

Comparison of different binders

Figure 13 compares the different binders considered: lime; activated ash; lime and ash; lime and activated ash; and OPC with RoadCem. As it was already observed in previous figures, the activated ash mixed with lime always showed the best performance, both in terms of final (28 days) strength and in terms of strength gain rate. Somehow surprisingly, the OPC + RoadCem mixture showed a rather slow strength increase, when compared with the remaining mixtures. However, it should be taken in consideration that the relative dosage might have a strong impact on these results, i.e., to have comparable strength values a higher dosage of OPC and RoadCem® might be necessary. On the other hand, the OPC content was already significant (8% and 12%), indicating that for the same strength values the use of alkali-activated ash may be more economic.

Conclusions

The paper compares the performance of different binders, based mainly on lime and fly ash, with or without alkaline activation as the liquid phase. It is highlighted that the alkaline activation reaction kinetics may be improved or reduced depending on the mixture composition. Lime, ash, sodium chloride and the alkaline activator were used in different combinations and compared to Portland cement and a specific new additive, recently available in the market for road applications. The following conclusions may be taken:

- The lime + activated ash mixtures were the most performing in terms of uniaxial compression strength and axial stiffness;
- The sodium chloride significantly improved the lime and lime-ash mixtures, but provided only a slight improvement in the activated ash mixtures;
- A 5% increase (from 10% to 15% in terms of solids weight) in lime content represented an important strength increase after 28 days, for the lime-based mixtures,

for the lime and no activated ash mixtures and for the lime and activated ash mixtures. Stress-strain curves and strength envelopes obtained in triaxial tests for the best performing mixtures (with lime and activated ash) showed a typical strong cemented soil behaviour with friction angles above 50º and cohesion intercepts higher than 500kPa.

- Considering the existing design guidelines for roads, the soil-lime mixtures studied in this work did not fulfil the necessary requirements, while the soil-lime-ash mixtures stay above the minimum values even without the activator. For higher performances, corresponding to higher-class treated layers as expressed in GTS (2000), activated ash mixtures are needed.

From the results obtained it is possible to conclude that alkali activated binders, based on low-calcium fly ash, can be very competitive with cement, regarding soil stabilisation for transport infrastructures applications. If the calcium content of the original fly ash is increased using an additional component like lime, not only the strength gain rate is enhanced, but the final strength is also improved.

Acknowledgments

The authors would like to acknowledge the company CJR Wind – Energy for life, for the funding which enable the presented research; the MCTES/FCT (Portuguese Science and Technology Foundation of Portuguese Ministry of Science and Technology) for their financial support through the SFRH/BPD/85863/2012 scholarship, which is co-funded by the European Social Fund by POCH program; and the Microscopy Unit of the University of Trás-os-Montes e Alto Douro. In addition, a special acknowledgment is also due to PEGOP – Energy Eléctrica, S.A. and LUSICAL – Companhia Lusitana de Cal, S.A. for providing respectively fly ash and lime for this study.

References

Al-Mukhtar, M., A. Lasledj & J. F. Alcover (2014). Lime consumption of different clayey soils. Applied Clay Science, 95,133-145. doi:10.1016/j.clay.2014.03.024

Arulrajah, A., Mohammadinia, A., Phummiphan, I., Horpibulsuk, S., & Samingthong, W. (2016). Stabilization of Recycled Demolition Aggregates by Geopolymers comprising Calcium Carbide Residue, Fly Ash and Slag precursors. Construction and Building Materials, 114, 864-873.

ASTM (2011). D 2487- 11: Standard Practice for Classification of Soils for Engineering Purposes (Unified Soil Classification System). Vol. 04.08. United States

ASTM (2015). C 618-15: Standard Specification for Coal Fly Ash and Raw or Calcined Natural Pozzolan for Use in Concrete. Vol. 04.02. United States

Bahar, R., M. Benazzoug & S. Kenai (2004). Performance of compacted cement-stabilised soil. Cement and Concrete Composites, 26(7), 811-820. doi:10.1016/j.cemconcomp.2004.01.003

Basha, E. A., Hashim, R., Mahmud H. B., Muntohar A. S. (2005). Stabilization of residual soil with rice husk ash and cement. Construction and Building Materials, 19(6), 448-453. doi:10.1016/j.conbuildmat.2004.08.001

Bui, P. T., Ogawa, Y., Nakarai K, Kawai K. (2015). Effect of internal alkali activation on pozzolanic reaction of low-calcium fly ash cement paste. Materials and Structures, 1-15. DOI 10.1617/s11527-015-0703-6

Camacho-Tauta, J. F., G. Cascante, A. Viana da Fonseca, and J. A. Santos. (2015). "Time and frequency domain evaluation of bender element systems." Géotechnique 65, no. 7 548-562.CEN (2003a). EN 13286-41 - Unbound and hydraulic bound mixtures. Test method for the determination of the compressive strength of hydraulically bound mixtures, Comité Européen de Normalisation, Bruxelles

CEN (2003b). EN 12504-4 Testing concrete – Part 4: Determination of ultrasonic pulse velocity. Comité Européen de Normalisation, Bruxelles

CEN (2004a). EN 13286-53 – Unbound and hydraulically bound mixtures – Part 53: Methods for the manufacture of test specimens of hydraulically bound mixtures using axial compression, Comité Européen de Normalisation, Bruxelles

CEN (2004b) ISO/TS 17892-9 – Geotechnical investigation and testing – Laboratory testing of soil – Part 9: Consolidated triaxial compression tests on water saturated soil, Comité Européen de Normalisation, Bruxelles

Consoli, N., Rosa, D.A., Cruz, R.C., Dalla-Rosa, A. (2011a). Water content, porosity and cement content as parameters controlling strength of artificially cemented silty soil, Engineering Geology, 122(3–4), 328–333. doi:10.1016/j.enggeo.2011.05.017

Consoli, N., Dalla-Rosa, A. & Saldanha, R. (2011b). Variables Governing Strength of Compacted Soil-Fly Ash-Lime Mixtures. Journal of Materials in Civil Engineering, 23(4), 432-440. doi: 10.1061/(ASCE)MT.1943-5533.0000186, 432-440.

Cristelo, N., Glendinning, S. & Jalali, S. (2009). Sub-Bases Layers of Residual Granite Soil Stabilised with Lime. Soils and Rocks, 32(2), 83-88

Cristelo, N., Glendinning, S. & Teixeira Pinto, A. (2011). Deep soft soil improvement by alkaline activation. Ground Improvement 164(GI2), 73-82. doi:10.1680/grim.900032

Cristelo, N., Glendinning, S., Miranda, T., Oliveira, D. and Silva, R. (2012a). Soil stabilisation using alkaline activation of fly ash for self-compacting rammed earth construction. Construction and Building Materials, 36, 727-735. doi:10.1016/j.conbuildmat.2012.06.037

Cristelo, N., Glendinning, S., Fernandes, L., Teixeira Pinto, A. (2012b). Effect of calcium content on soil stabilisation with alkaline activation. Construction and Building Materials, 29, 167-174. doi:10.1016/j.conbuildmat.2011.10.049

Cristelo, N., Glendinning, S., Fernandes, L., Teixeira Pinto, A. (2013). Effects of alkaline-activated fly ash and Portland cement on soft soil stabilization. Acta Geotechnica, 8, 395-405. doi: 10.1007/s11440-012-0200-9

Cristelo, N., Miranda, T., Oliveira, D.V., Rosa, I., Soares, E., Coelho, P., Fernandes, L. (2015). Assessing the production of jet mix columns using alkali activated waste based on mechanical and financial performance and CO2 (eq) emissions. Journal of Cleaner Production, 102, 447-460. doi:10.1016/j.jclepro.2015.04.102

Dombrowski, K., Buchwald, A. & Weil, M. (2006). The influence of calcium content on the structure and thermal performance of fly ash based geopolymers. Journal of Materials Science, 42(9), 3033-3043. doi: 10.1007/s10853-006-0532-7

Elkady, T.Y. (2016). The effect of curing conditions on the unconfined compression strength of lime-treated expansive soils, Road Materials and Pavement Design, 17(1), 52-69, doi: 10.1080/14680629.2015.1062409

Fernandez, A. and J. Santamarina (2001). Effect of cementation on the small-strain parameters of sands. Canadian Geotechnical Journal, 38(1), 191-199. doi:10.1139/t00-081

Fernández-Jiménez, A. & Palomo, A. (2005). Composition and microstructure of alkali activated fly ash binder:Effect of the activator. Cement and Concrete Research,35, 1984–1992. doi:10.1016/j.cemconres.2005.03.003

568 Fernández-Jiménez, A., de la Torre, A.G., Palomo, A., López-Olmo, G., Alonso, M.M.,
569 Aranda, M. a. G. (2006). Quantitative determination of phases in the alkaline
570 activation of fly ash. Part II: Degree of reaction. Fuel, 85, 1960–1969
571 doi:10.1016/j.fuel.2006.04.006
572 García Lodeiro, I., D. E. Macphee, A. Palomo and A. Fernández-Jiménez (2009). Effect of
573 alkalis on fresh C–S–H gels. FTIR analysis. Cement and Concrete Research, 39(3):
574 147-153. doi: 10.1016/j.cemconres.2009.01.003
575 Garcia-Lodeiro, I., A. Palomo, A. Fernández-Jiménez and D. E. Macphee (2011).
576 Compatibility studies between N-A-S-H and C-A-S-H gels. Study in the ternary
577 diagram Na2O–CaO–Al2O3–SiO2–H2O. Cement and Concrete Research, 41(9): 923-
578 931. doi:10.1016/j.cemconres.2011.05.006
579 Garcia-Lodeiro I, Fernandez-Jimenez A and Palomo A. (2013). Variation in hybrid cements
580 over time. Alkaline activation of fly ash-Portland cement blends. Concrete Research,,
581 52,112-122. http://dx.doi.org/10.1016/j.cemconres.2013.03.022
582 Ghosh, A., & Subbarao, C. (2001). Microstructural development in fly ash modified with lime
583 and gypsum. Journal of Materials in Civil Engineering, 13(1), 65–70
584 doi:10.1061/(ASCE)0899-1561(2001)13:1(65), 65-70.
585 Goodary, R., Lecomte-Nana, G. L., Petit C., Smith D. S. (2012). Investigation of the strength
586 development in cement-stabilised soils of volcanic origin. Construction and Building
587 Materials, 28(1), 592-598. doi:10.1016/j.conbuildmat.2011.08.054
588 Goto, S., Tatuoka, F. Shibuya, S., Kim, Y.S and Sato, T. (1991). A simple gauge for local
589 small strain measurements in the laboratory. Soil and Foundations, 31(1), 169-180.
590 doi: 10.3208/sandf1972.31.169
591 GTS (2000). Guide technique pour le traitement des sols à la chaux et/ou aux liants
592 hydrauliques. Application à la réalisation des remblais et des couches de forme.
593 (Technical guide for soils treated with lime and cement, In French), LCPC/SETRA.
594 Güllü, H. (2015). Unconfined compressive strength and freeze–thaw resistance of fine-
595 grained soil stabilised with bottom ash, lime and superplasticiser, Road Materials and
596 Pavement Design, 16(3), 608-634, doi: 10.1080/14680629.2015.1021369
597 Gurbuz, A. (2015). Marble powder to stabilise clayey soils in sub-bases for road construction,
598 Road Materials and Pavement Design, 16(2), 481-492,
599 doi:10.1080/14680629.2015.1020845

600 Han, C. & Cheng, P. (2015). Micropore variation and particle fractal representation of lime-
601 stabilised subgrade soil under freeze–thaw cycles, Road Materials and Pavement
602 Design, 16(1), 19-30, doi:10.1080/14680629.2014.956139
603 Hoy, M., Horpibulsuk, S., & Arulrajah, A. (2016). Strength development of Recycled Asphalt
604 Pavement–Fly ash geopolymer as a road construction material. Construction and
605 Building Materials, 117, 209-219.
606 Horpibulsuk, S., Katkan, W., Sirilerdwattana, W., Rachan R. (2006). Strength development in
607 cement stabilized low plasticity and coarse grained soils: laboratory and field study.
608 Soils and Foundations, 46(3), 351-366. doi: 10.3208/sandf.46.351
609 Ingles, O. G. & Metcalf, J. B. 1972. Soil stabilization: principles and practice. Butterworths,
610 Sydney – Melbourne – Briesbane.
611 JAE (1995). Pavement design manual for the national road network. Junta Autónoma de
612 Estradas (in Portuguese)
613 Juenger, M. C. G., Winnefeld, F., Provis, J. L., Ideker J. H. (2011). Advances in alternative
614 cementitious binders. Cement and Concrete Research, 41(12), 1232-1243.
615 doi:10.1016/j.cemconres.2010.11.012
616 Kamei, T., Ahmed A. & Ugai K. (2013). Durability of soft clay soil stabilized with recycled
617 Bassanite and furnace cement mixtures. Soils and Foundations, 53(1), 155-165.
618 doi:10.1016/j.sandf.2012.12.011
619 Kaniraj, S. R. and Havanagi, V. G. (1999). Compressive strength of cement stabilized fly ash-
620 soil mixtures. Cement and Concrete Research, 29(5), 673-677. doi:10.1016/S0008-
621 8846(99)00018-6
622 Khemissa, M. & A. Mahamedi (2014). Cement and lime mixture stabilization of an expansive
623 overconsolidated clay. Applied Clay Science, 95, 104-110.
624 doi:10.1016/j.clay.2014.03.017
625 Kolias, S., Kasselouri-Rigopoulou V. & Karahalios A. (2005). Stabilisation of clayey soils
626 with high calcium fly ash and cement. Cement and Concrete Composites, 27(2), 301-
627 313. doi:10.1016/j.cemconcomp.2004.02.019
628 Kua, T. A., Arulrajah, A., Horpibulsuk, S., Du, Y. J., & Shen, S. L. (2016). Strength
629 assessment of spent coffee grounds-geopolymer cement utilizing slag and fly ash
630 precursors. Construction and Building Materials, 115, 565-575.
631 Kumar, A., Walia, B., & Bajaj, A. (2007). Influence of Fly Ash, Lime, and Polyester Fibers
632 on Compaction and Strength Properties of Expansive Soil. Journal of Materials in

633 Civil Engineering, 19(3), 242-248, doi: 10.1061/(ASCE)0899-1561(2007)19:3(242),
634 242-248
635 Little and Nair (2009). Recommended practice for stabilization of subgrade soils and base
636 materials. National Cooperative Highway Research Program, Transportation Research
637 Board of National Academies, USA
638 Little, D. (1995). Handbook for stabilisation of pavement subgrades and base courses with
639 lime. Lime association of Texas, USA
640 Little, D., Nair, S., & Herbert, B. (2010). Addressing Sulfate-Induced Heave in Lime Treated
641 Soils. Journal of Geotechnical and Geoenvironmental Engineering,
642 doi:10.1061/(ASCE)GT.1943-5606.0000185, 110-118.
643 Marjanovic, P., Egyed, C.E.G., de La Roij, P. and de La Roij, R. (2009). The Road to the
644 Future. Manual Working with RoadCem. PowerCem Technologies B.V. The
645 Netherlands
646 Mitchell, J. (1981). Soil-improvement - State-of-the-art report. Proc. 10th ICSMFE,
647 Stockholm.
648 Mohammadinia, A., Arulrajah, A., Sanjayan, J., Disfani, M., Bo, M., and Darmawan, S.
649 (2014). "Laboratory Evaluation of the Use of Cement-Treated Construction and
650 Demolition Materials in Pavement Base and Subbase Applications." J. Mater. Civ.
651 Eng., 10.1061/(ASCE)MT.1943-5533.0001148, 04014186.
652 Narendra, B. S., Sivapullaiah P. V. & Ramesh H. N. (2003). Optimum lime content of fly ash
653 with salt. Proc. of the Inst. of Civil Engineers - Ground Improvement, 7(4), 187-191.
654 doi: 10.1680/grim.2003.7.4.187
655 Oza, J. B. & Gundaliya, P. J. (2013). Study of Black Cotton Soil Characteristics with Cement
656 Waste Dust and Lime. Procedia Engineering 51: 110-118.
657 doi:10.1016/j.proeng.2013.01.017
658 Petry, T. & Little, D. (2002). Review of Stabilization of Clays and Expansive Soils in
659 Pavements and Lightly Loaded Structures—History, Practice, and Future. J. Mater.
660 Civ. Eng., 10.1061/(ASCE)0899-1561(2002)14:6(447), 447-460.
661 Phetchuay, C., Horpibulsuk, S., Suksiripattanapong, C., Chinkulkijniwat, A., Arulrajah, A., &
662 Disfani, M. M. (2014). Calcium carbide residue: Alkaline activator for clay–fly ash
663 geopolymer. Construction and Building Materials, 69, 285-294.
664 Phummiphan, I., Horpibulsuk, S., Sukmak, P., Chinkulkijniwat, A., Arulrajah A., Shen S.-L.
665 (2016). Stabilisation of marginal lateritic soil using high calcium fly ash-based

666 geopolymer. Road Materials and Pavement Design.
667 doi:10.1080/14680629.2015.1132632
668 Provis, J., van Deventer, J. (Eds.) (2014). Alkali Activated Materials: State-of-the-art Report,
669 RILEM TC 224-AAM. Springer
670 Puligilla, S. & Mondal, P. (2013). Role of slag in microstructural development and hardening
671 of fly ash-slag geopolymer. Cement and Concrete Research, 43, 70-80.
672 doi:10.1016/j.cemconres.2012.10.004
673 Ramesh H. N., Sivapullaiah, P. V. & Sivamohan, M. (1999). lmprovement of strength of fly
674 ash with lime and sodium salts. Proc. of the Inst. of Civil Engineers - Ground
675 Improvement, 3, 163-167.
676 Rao, S. & P. Acharya (2014). Synthesis and Characterization of Fly Ash Geopolymer Sand.
677 Journal of Materials in Civil Engineering, 26(5), 912-917.
678 doi:10.1061/(ASCE)MT.1943-5533.0000880
679 Rios, S., Viana da Fonseca, A. & Baudet, B. (2012). The effect of the porosity/cement ratio
680 on the compression behaviour of cemented soil. Journal of Geotechnical and
681 Environmental Engineering, 138(11), 1422–1426, doi: 10.1061/(ASCE)GT.1943-
682 5606.0000698
683 Rios, S., Viana da Fonseca, A. and Baudet, B. (2014). On the shearing behaviour of an
684 artificially cemented soil. Acta Geotechnica, 9(2), 215-226, doi : 10.1007/s11440-013-
685 0242-7
686 Rios, S., Cristelo, C., Viana da Fonseca, A., Ferreira, C. (2015). Structural Performance of
687 Alkali Activated Soil-Ash versus Soil-Cement. Journal of Materials in Civil
688 Engineering, doi: 10.1061/(ASCE)MT.1943-5533.0001398.
689 Samaras, P., Papadimitriou, C. A., Haritou, I., Zouboulis, A. I. (2008). Investigation of
690 sewage sludge stabilization potential by the addition of fly ash and lime. Journal of
691 Hazardous Materials 154(1-3), 1052-1059
692 Saride, S., Puppala, A. J. & Chikyala, S. R. (2013). Swell-shrink and strength behaviors of
693 lime and cement stabilized expansive organic clays. Applied Clay Science, 85, 39-45.
694 doi:10.1016/j.clay.2013.09.008
695 Saride, S., Avirneni, D., & Challapalli, S. (2016). Micro-mechanical interaction of activated
696 fly ash mortar and reclaimed asphalt pavement materials. Construction and Building
697 Materials, 123, 424-435.

698 Scrivener, K.L., Kirkpatrick, R.J. (2008). Innovation in use and research on cementitious
699 material. Cement and Concrete Research, 38, 128-136
700 doi:10.1016/j.cemconres.2007.09.025
701 Sherwood, P. (1993). Soil stabilization with cement and lime. State of the Art Review.
702 London: Transport Research Laboratory, HMSO
703 Silva, R.A., Oliveira, D.V., Miranda, T., Cristelo, N., Escobar, M.C., Soares, E. (2013).
704 Rammed earth construction with granitic residual soils: The case study of northern
705 Portugal. Construction and Building Materials, 47(0), 181-191.
706 doi:10.1016/j.conbuildmat.2013.05.047
707 Sukmak, P., Horpibulsuk S., & Shen S.-L (2013). Strength development in clay–fly ash
708 geopolymer. Construction and Building Materials, 40(0), 566-574.
709 doi: 10.1016/j.conbuildmat.2012.11.015
710 Sukmak, P., P. D. Silva, S. Horpibulsuk and P. Chindaprasirt (2015). Sulfate Resistance of
711 Clay-Portland Cement and Clay High-Calcium Fly Ash Geopolymer. Journal of
712 Materials in Civil Engineering 27(5): 04014158.
713 Van Impe, W.F. (1989). Soil improvement techniques and their evolution, Rotterdam,
714 Balkema, Netherlands
715 Xing, H. F., Yang, X. M, Xu, C. and Ye, G. B. (2009). Strength characteristics and
716 mechanisms of salt-rich soil-cement, Engineering Geology, 103 33–38, doi:
717 http://dx.doi.org/10.1016/j.enggeo.
718 Yi, Y., C. Li and S. Liu (2015). "Alkali-Activated Ground-Granulated Blast Furnace Slag for
719 Stabilization of Marine Soft Clay." Journal of Materials in Civil Engineering 27(4):
720 04014146.
721 Yilmaz, Y. & V. Ozaydin (2013). Compaction and shear strength characteristics of
722 colemanite ore waste modified active belite cement stabilized high plasticity soils.
723 Engineering Geology, 155, 45-53. doi:10.1016/j.enggeo.2013.01.003
724 Yong, R. N. & Ouhadi, V. R. (2007). Experimental study on instability of bases on natural
725 and lime/cement-stabilized clayey soils. Applied Clay Science, 35(3–4), 238-249.
726 doi:10.1016/j.clay.2006.08.009
727 Yusuf, F., Little, D. N., & Sarkar, S. L. (2001). Evaluation of structural contribution of lime
728 stabilization of subgrade soils in Mississippi. Transportation Research Record 1757,
729 Transportation Research Board, National Research Council, Washington DC, 22–31

730 Zhang, M., Guo, H., El-Korchi, T., Zhang, G. & Tao, M. (2013). Experimental feasibility
731 study of geopolymer as the next-generation soil stabilizer. Construction and Building
732 Materials, 47(0), 1468-1478. doi: 10.1016/j.conbuildmat.2013.06.017
733

734 **List of Figures**

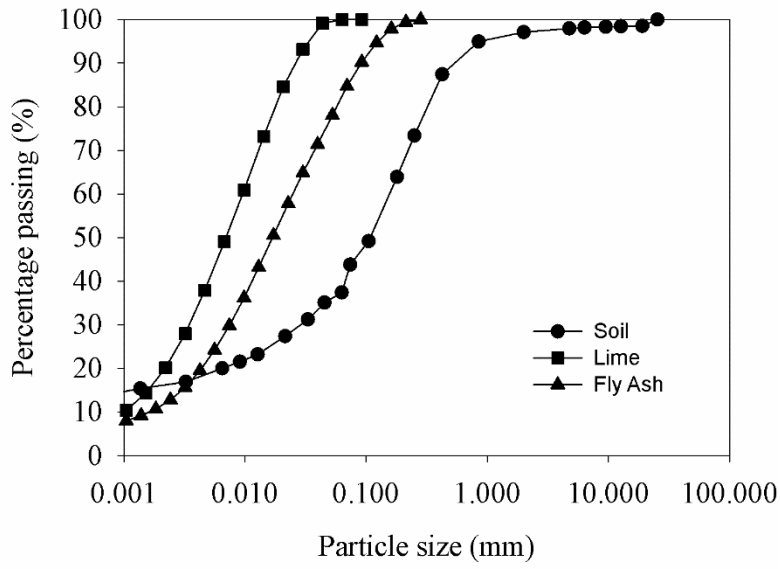

735

736 Figure 1 - Particle size distribution of the soil, lime and fly ash

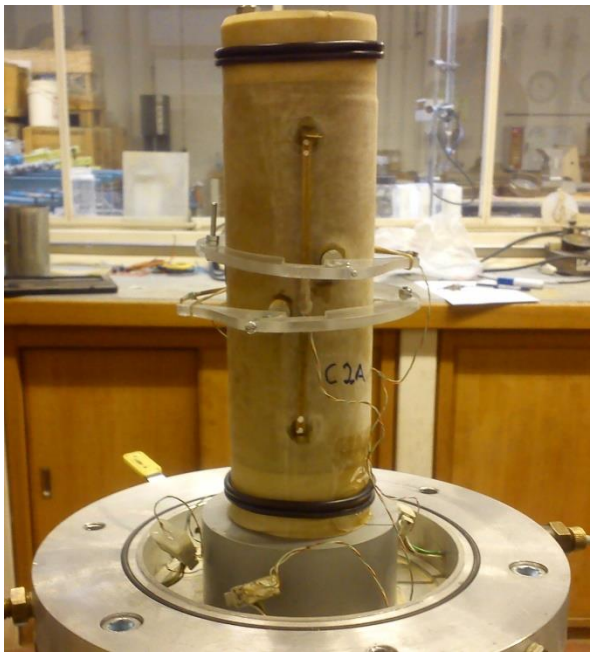

737

738 Figure 2 - Triaxial test setup showing the Linear Displacement Transformers (LDT) sensors

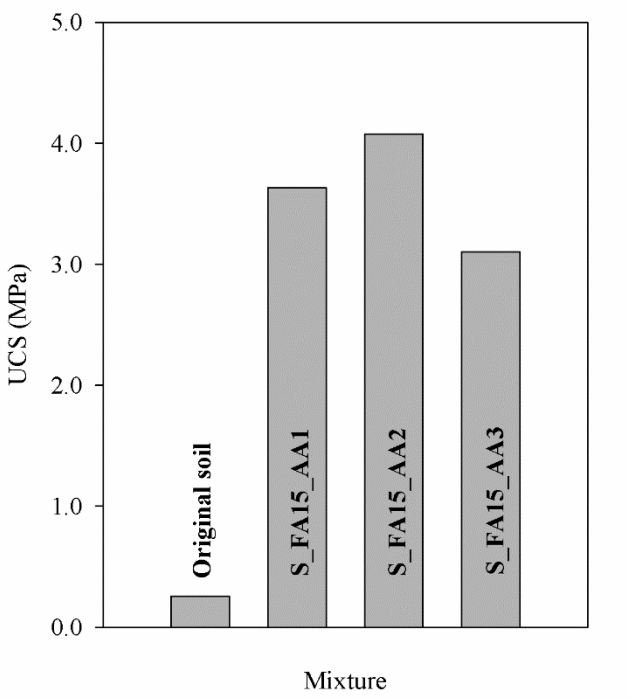

739

740 Figure 3 - Step 1 UCS results (28 days curing)

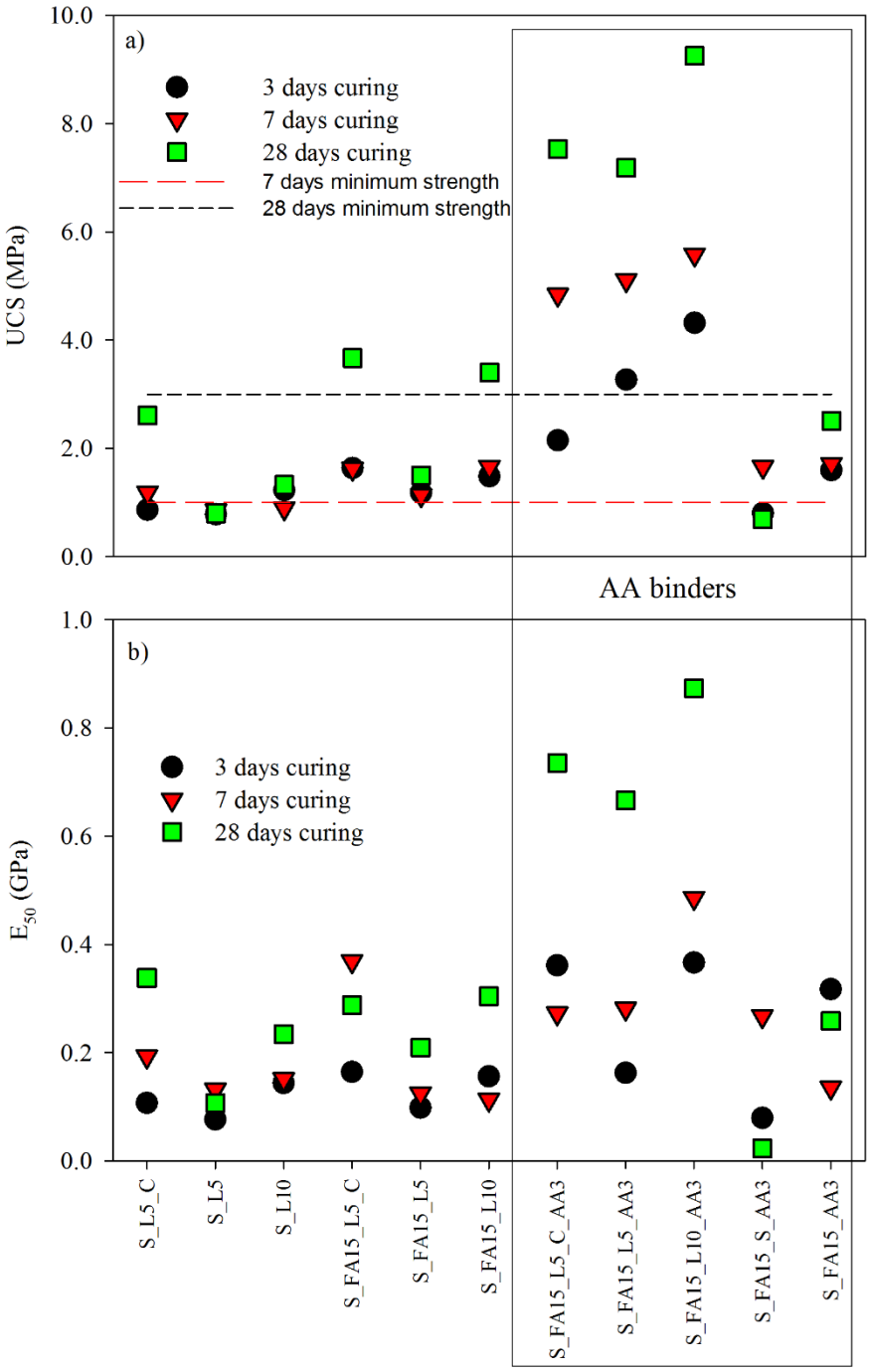

741

742 Figure 4 - UCS results for step 2 (3, 7 and 28 days curing): a) unconfined compressive
743 strength (UCS); b) Stiffness modulus at 50% of maximum strength (E_{50}) - S (soil); FA (fly
744 ash); L (lime); C (sodium chloride); AA (alkali activated)

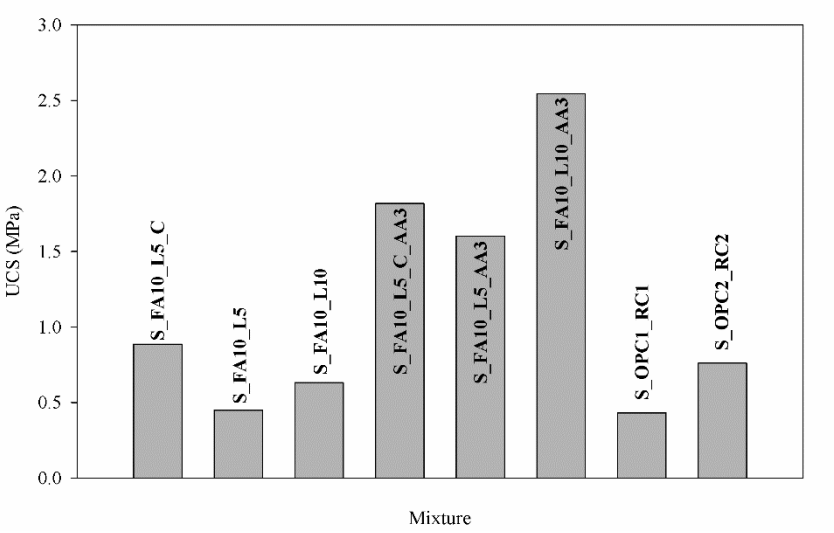

745

746 Figure 5 - UCS results for step 3 (7 days curing) - S (soil); FA (fly ash); L (lime); C (sodium
747 chloride); AA (alkali activated); OPC (Portland cement); RC (RoadCem)

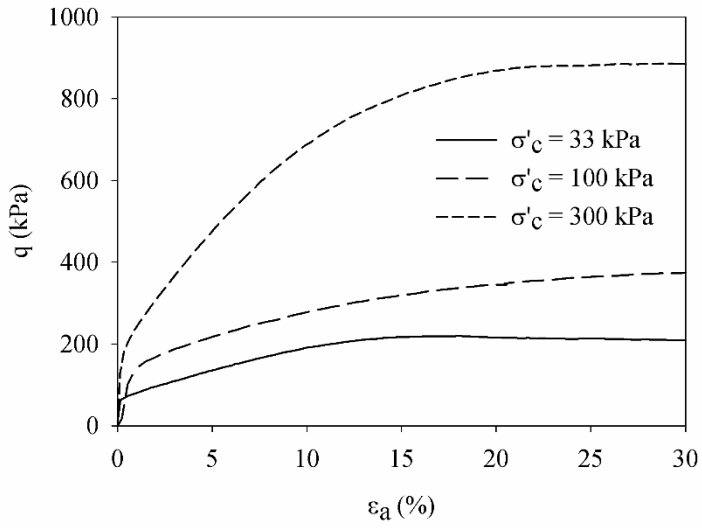

748

749 Figure 6 - Stress-strain curves obtained from the triaxial compression tests performed on the
750 original soil (σ'c refers to the isotropic consolidation stress applied)

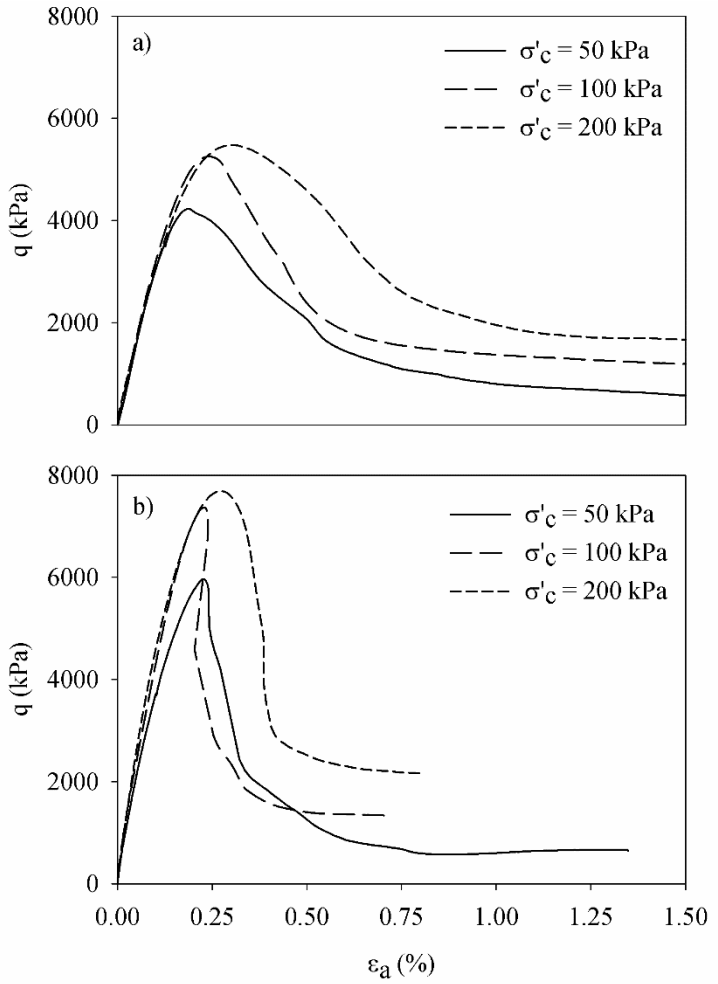

751

752 Figure 7 - Stress-strain curves obtained from the triaxial compression tests performed on the
753 mixtures S_FA10_L5_AA3 (a) and S_FA15_L5_AA3 (b) (σ'c refers to the isotropic
754 consolidation stress applied)

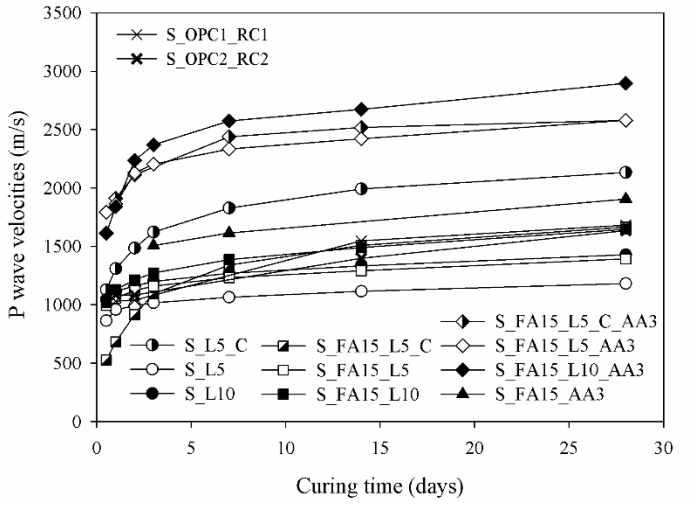

755

756 Figure 8 – P wave velocities evolution with curing time

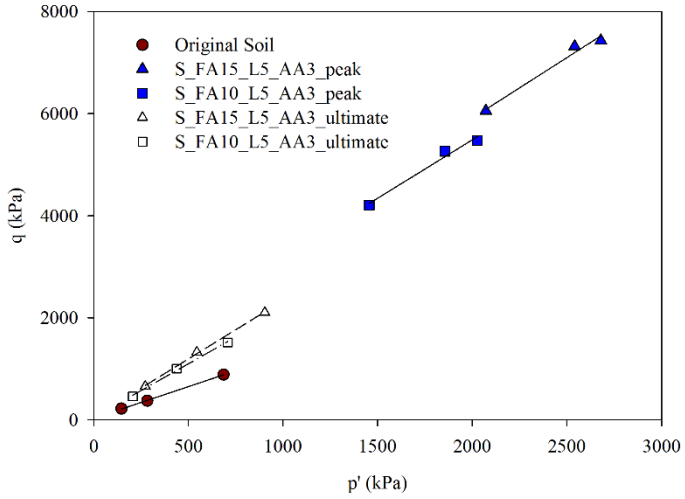

757

758 Figure 9 - Peak and ultimate state strength envelopes (the soil specimens presented very

759 similar peak and ultimate envelops, which are not possible to distinguish at this scale)

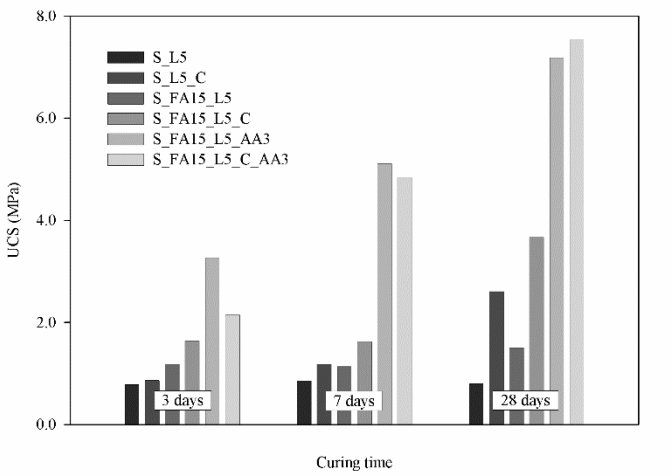

760

761 Figure 10 - Effect of sodium chloride on the uniaxial compression strength

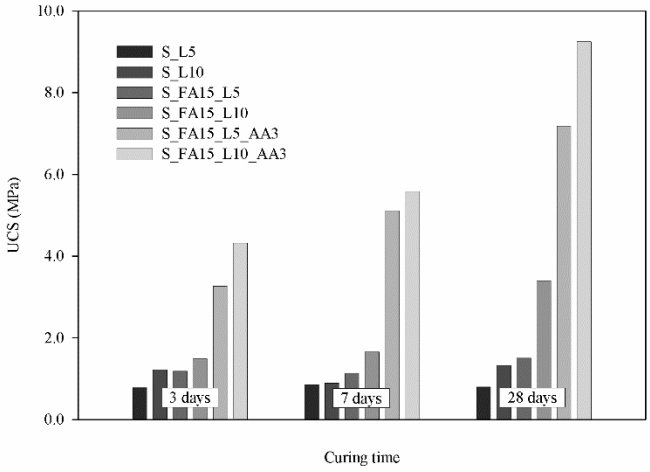

762

763 Figure 11 - Effect of lime percentage on the uniaxial compression strength

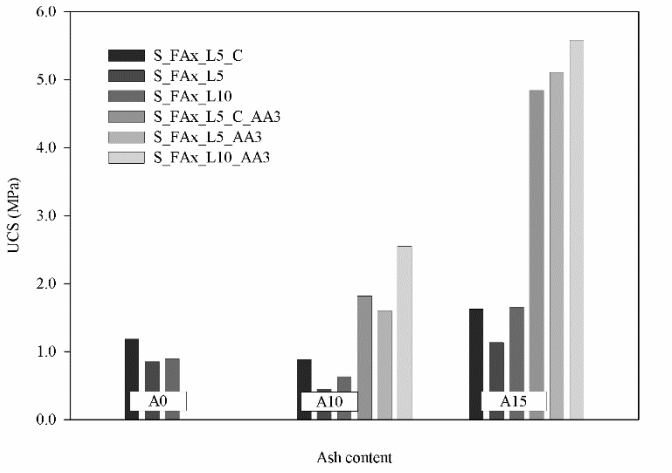

764

765 Figure 12 - Effect of ash percentage on the uniaxial compression strength after curing for 7
766 days

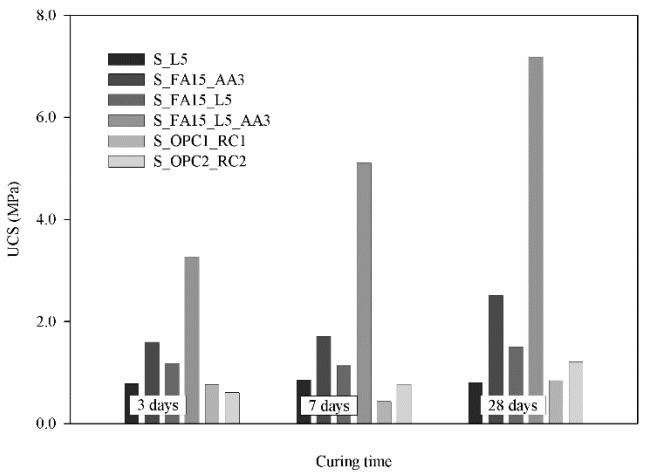

767

768 Figure 13 – Effect of the binder type on the uniaxial compression strength

769

770

771

List of Tables

Table 1 - Main geotechnical properties of the soil

Properties	Symbol	Value
Plastic limit (%)	w_P	13.0
Liquid limit (%)	w_L	19.5
Average diameter (mm)	D_{50}	0.105
Fines fraction (sieve Nº 200) (%)	$P_{\#200}$	43.8
Uniformity coefficient	C_u	167
Curvature coefficient	C_c	6.7
Specific gravity	G	2.60
Modified Proctor test optimum water content (%)	w_{op}	8.2
Modified Proctor test maximum density (kN/m3)	γ_d	21.29
California Bearing Ratio (%)	CBR	9
Unified Soil Classification System ASTM D 2487 (2011)	-	SC-SM silty sand

Table 2: Chemical composition of the fly ash (wt%)

Element	Si	Al	Fe	Ca	K	Ti	Mg	Na	S	P
Fly ash	48.81	21.77	14.74	3.85	4.42	1.79	1.56	1.31	1.17	0.58

Table 3 - Identification of prepared mixtures

Step	ID	Solid Phase				Liquid Phase	
		Soil (%)	Ash (%)	Lime (%)	SC(*) (%)	Activator/ Fly ash (wt)	Water content (%)
0	Soil	100	-	-	-	-	5.0
1	S_FA15_AA1	85	15	-	-	0.943	10.4
	S_FA15_AA2	85	15	-	-	0.825	9.1
	S_FA15_AA3	85	15	-	-	0.707	7.8
2	S_L5_C	94	-	5	1	-	5.0
	S_L5	95	-	5	-	-	5.0
	S_L10	90	-	10	-	-	5.0
	S_FA15_L5_C	79	15	5	1	-	5.0
	S_FA15_L5	80	15	5	-	-	5.0
	S_FA15_L10	75	15	10	-	-	5.0
	S_FA15_C_AA3	84	15	-	1	0.707	7.8
	S_FA15_AA3	85	15	-	-	0.707	7.8
	S_FA15_L5_C_AA3	79	15	5	1	0.707	7.8
	S_FA15_L5_AA3	80	15	5	-	0.707	7.8
	S_FA15_L10_AA3	75	15	10	-	0.707	7.8
3	S_FA10_L5_C	84	10	5	1	-	5.0
	S_FA10_L5	85	10	5	-	-	5.0
	S_FA10_L10	80	10	10	-	-	5.0
	S_FA10_L5_C_AA3	84	10	5	1	1.06	7.8
	S_FA10_L5_AA3	85	10	5	-	1.06	7.8
	S_FA10_L10_AA3	80	10	10	-	1.06	7.8
	S_OPC1_RC1	92	8% OPC + 0.08% RC			-	5.0
	S_OPC2_RC2	88	12% OPC + 0.11% RC			-	5.0

(*) SC stands for sodium chloride

782 Table 4 – Tests performed in each mixture and corresponding curing time

Step	ID	Curing time of the specimens tested in:		
		UCS	Triaxial tests	Seismic waves
0	Soil	0	0	
1	S_FA15_AA1	28		
	S_FA15_AA2	28		
	S_FA15_AA3	28		
2	S_L5_C	3, 7, 28		12, 24 and 48 h + 3, 7, 14 and 28 days
	S_L5	3, 7, 28		12, 24 and 48 h + 3, 7, 14 and 28 days
	S_L10	3, 7, 28		12, 24 and 48 h + 3, 7, 14 and 28 days
	S_FA15_L5_C	3, 7, 28		12, 24 and 48 h + 3, 7, 14 and 28 days
	S_FA15_L5	3, 7, 28		12, 24 and 48 h + 3, 7, 14 and 28 days
	S_FA15_L10	3, 7, 28		12, 24 and 48 h + 3, 7, 14 and 28 days
	S_FA15_C_AA3	3, 7, 28		
	S_FA15_AA3	3, 7		12, 24 and 48 h + 3, 7, 14 and 28 days
	S_FA15_L5_C_AA3	3, 7, 28		12, 24 and 48 h + 3, 7, 14 and 28 days
	S_FA15_L5_AA3	3, 7, 28	28	12, 24 and 48 h + 3, 7, 14 and 28 days
	S_FA15_L10_AA3	3, 7, 28		12, 24 and 48 h + 3, 7, 14 and 28 days
3	S_FA10_L5_C	7		
	S_FA10_L5	7		
	S_FA10_L10	7		
	S_FA10_L5_C_AA3	7		
	S_FA10_L5_AA3	7	28	
	S_FA10_L10_AA3	7		
	S_OPC1_RC1	3, 7, 28		12, 24 and 48 h + 3, 7, 14 and 28 days
	S_OPC2_RC2	3, 7, 28		12, 24 and 48 h + 3, 7, 14 and 28 days

783

784 Table 5 - Stiffness modulus at 50% of the deviatoric stress (E_{50}). Results in MPa

Mixture	Confining pressure of 33 (soil) or 50 kPa (mixtures)	Confining pressure of 100 kPa	Confining pressure of 300 (soil) or 200 kPa (mixtures)
Soil	3.68	6.84	10.21
S_FA10_L5_AA3	3194.3	3299.7	3154.3
S_FA15_L5_AA3	3901.1	4392.1	4759.9

785

786 Table 6 – Mohr Coulomb failure criteria parameters

Mixture	Peak		Ultimate strength	
	ϕ' (○)	c' (kPa)	ϕ' (○)	c' (kPa)
Soil	31	15	32	0
S_FA10_L5_AA3	56	587	49	27
S_FA15_L5_AA3	58	796	56	33

787